Estimation of the Mean Grain Size of Mechanically Induced Hydroxyapatite Based Bioceramics via Artificial Neural Network

Mohammad Fahami [1], Majid Abdellahi[2,*]

[1] *Department of Mechanical Engineering, Najafabad Branch, Islamic Azad University, Najafabad, Iran*
[2] *Advanced Materials Research Center, Department of Materials Engineering, Najafabad Branch, Islamic Azad University, Najafabad, Iran*

ARTICLE INFO

Article history:

Received 17 November 2016
Accepted 4 February 2017
Available online 25 June 2017

Keywords:

Artificial neural network
Mechanical alloying
Hydroxyapatite
Bioceramics

ABSTRACT

This study focuses on the estimation of the mean grain size of mechanically induced Hydroxyapatite (HA) through the artificial neural network (ANN) model. The mean grain size of HA and HA based nanocomposites at different milling parameters was obtained from previous studies. The data were trained and tested by the neural network modeling. Accordingly, all data (55 sets) were based on mechanical alloying and were randomly divided into 40 training sets and 15 testing sets. The data used in the multilayer feed forward neural networks models and input variables of models were arranged in a format of 13 input parameters. The results indicated a very good agreement between the experimental data and the predicted ones. The R^2 value of the trained and tested data suggested by the model confirmed this situation. Given the broad range of the used parameters, it was found that our analysis and model were fully functional to accurately estimate the optimal conditions for experiments. This shows the potential application of these calculations and analyses in a wide range of numerical studies.

1-Introduction

Boiler components, such as main steam piping and the header parts of boilers, are usually exposed to high thermal stresses. A387-Gr.91steel is one of the suitable candidates for the mentioned application that explores good creep and fatigue resistance [1]. In other words, due to high corrosion, oxidation and creep resistance of austenitic stainless steels, super-heater and re-heater parts are made of these alloys [1, 2].

The welding of these two dissimilar steels by different welding routes has been the subject of wide research. Usually, the shielded metal arc welding (SMAW) and gas tungsten arc welding (GTAW) processes are applied to weld these alloys. The major problem encountered with the using of austenitic stainless steels as filler metals is possible carbon migration from ferritic steel to the welding metal and brittleness of the weld especially in the service temperatures more than 315°C. Welding of parts like tubes in the boiler that are in contact with the sulfurous environment by nickel-base fillers such as ERNiCrMo-3 is one solution to overcome the problem [3, 4, 5].

GTAW process is one of the fusion welding routes used in dissimilar welding of ferritic steels to austenitic stainless steels. Because of solidification structure, mechanical properties and corrosion resistance of the welding metal decline and it is possible to be modified by

* Corresponding author:
E-mail address: abdellahi@pmt.iaun.ac.ir

Mechanical alloying (MA) is a solid state technique used for making of nanocrystalline alloys, bioceramics, and intermetallic compounds. MA allows materials scientists to dominate material restriction and prepare alloys that are difficult or impossible to be synthesized by conventional melting and casting techniques [1]. This technique involves repeated deformation, welding and fracturing of powder particles [2]. A growing demand for the adjustment of the properties of novel materials produced by MA to certain applications and also the development of the MA regimes and apparatus designs for commercial scaling necessitate the development of mathematical models of MA [3]. The first modeling of mechanical alloying was carried out by Volin and Benjamin [3].

Artificial neural network (ANN) is one of the most powerful modeling techniques in conjunction with the statistical approach, which seems quite suitable for the estimation of mechanical alloying outputs. The neural network theory deals with learning from a previous obtained data, which is called the training or learning set, and then to check the system success using test data [4]. Over recent years the interest in the ANN modeling in different fields of materials science has increased [5]. The advantages of ANN modeling are based on reduction of time and cost in all the required experimental activities. This technique essentially involves the interconnection of simple computational elements known as neurons or nodes [6].

Hydroxyapatite (HA) as an inorganic component of bone and teeth is commonly used to coat metallic implants and to repair bone defects due to its excellent biocompatibility, osteoconductivity, and bioactivity. This class of ceramics are potential candidates to be used in the manufacturing of bone-like scaffolds and may also be designed in surgery for the reconstruction of bone defects [7, 8] . With the development of artificial intelligence theory, the estimation in non-linear problems has become an effective technique. Altinkok and Koker [9] reported a new design of a neural network to estimate the percentage of alumina in Al_2O_3/SiC and the pore volume fraction in a ceramic cake for any given amount of reinforcement (SiC) in the mixture. Moreover, in another research they designed a neural network to predict the density properties and tensile strengths in particle reinforced aluminum matrix composites based on given SiC particle size [10]. However, information regarding the prediction of the mean grain size of mechanically induced HA and HA based nanocomposites is limited. This research aims at designing an ANN modeling of mechanically induced HA and HA based nanocomposites to predict the mean grain size of the product under different conditions. In this relation, the milling and reaction parameters, including different percentages of reinforcement, ball to powder ratio (BPR), crystallinity degree, lattice strain, different percentages of matrix, different atmospheres, milling time, different revolutions per minute (RPM), various heat treatment temperatures, different types of ball mills as well as variety of balls and jars were employed as the input parameters in this model.

2- Experimental

The collected data from the previous works [11–22] are listed in Table 1. The input parameters consisted of different percentages of reinforcement, ball to powder ratio (BPR), crystallinity degree, lattice strain, different percentages of matrix, different atmospheres, milling time, revolutions per minute (RPM), different annealing temperatures, the type of balls and jars, with the ranges given in Table 1. Some symbols and reaction description of the materials presented in Table 1 are presented in Table 2.

3- Artificial neural networks

ANN is best explained as a set of simple highly interconnected processing elements that are capable of learning the information presented to them. The neural network theory is based on the studies of biological activities of the brain, which were developed to model the human brain [23]. McCulloch and Pitts [24] reported artificial neurons for the first time and developed a neuron model. Rosenblatt [25] designed a machine called perceptron that performed much in the same way as the human mind. Rumelhart et al. [26] developed a learning algorithm for perceptron networks with constituted hidden units.

Table1. The gathered data as input and target for training and testing sets from the previous works (using Planetary Ball Mill Type).

Matrix	Reinforcement	Amount of reinforcement%	Type of vial	Type of ball	RPM	BPR	Milling atmosphere	T (°C)	Milling time	Mean grain size(nm)	Elasticity	Crystallinity (X_c)	Ref
HA-R1	TiO2	20	Polyamide	ZrO_2	600	20:1	Air	25	40	37	0.31	80	[11]
HA-R1	TiO2	20	Polyamide	ZrO_2	600	20:1	Ar	25	40	37	0.3	76	[11]
HA-R1	TiO2	20	Polyamide	ZrO_2	600	20:1	Air	25	80	32	0.35	96	[11]
HA-R1	TiO2	20	Polyamide	ZrO_2	600	20:1	Ar	25	80	32	0.37	98	[11]
HA-R2	TiO2	20	Polyamide	ZrO_2	600	20:1	Air	25	40	34	0.33	82	[11]
HA-R2	TiO2	20	Polyamide	ZrO_2	600	20:1	Ar	25	40	40	0.28	70	[11]
HA-R2	TiO2	20	Polyamide	ZrO_2	600	20:1	Air	25	80	27	0.42	92	[11]
HA-R2	TiO2	20	Polyamide	ZrO_2	600	20:1	Ar	25	80	33	0.3	15	[11]
HA-R3	Ti	20	Polyamide	ZrO_2	600	20:1	Ar	25	10	20.13	0.621	17	[12]
HA-R3	Ti	20	Polyamide	ZrO_2	600	20:1	Ar	25	15	19.06	0.601	15	[12]
HA-R3	Ti	20	Polyamide	ZrO_2	600	20:1	Ar	25	20	13.13	0.530	13	[12]
HA-R3	Ti	20	Polyamide	ZrO_2	600	20:1	Ar	650	10	28.9	0.376	80	[12]
HA-R3	Ti	20	Polyamide	ZrO_2	600	20:1	Ar	650	15	26.6	0.407	65	[12]
HA-R3	Ti	20	Polyamide	ZrO_2	600	20:1	Ar	650	20	29.86	0.365	69	[12]
HA-R3	TiO2 + Mg	20	Polyamide	ZrO_2	600	20:1	Air	25	10	24.4	0.527	48	[13]
HA-R3	TiO2 + Mg	20	Polyamide	ZrO_2	600	20:1	Air	700	10	34.4	0.377	80	[13]
TCP	TiO2 + Mg	20	Polyamide	ZrO_2	600	20:1	Air	900	10	43.3	0.339	88	[13]
TCP	TiO2 + Mg	20	Polyamide	ZrO_2	600	20:1	Air	1100	10	51.9	0.268	94	[13]
A-TCP-R1	F	20	Steel	Steel	600	20:1	Air	25	10	20	0.83	22	[14]
A-TCP-R2	F	20	Steel	Steel	600	20:1	Air	25	10	69	0.58	65	[14]
A-TCP-R3	F	20	Steel	Steel	600	20:1	Air	25	10	58	0.64	57	[14]
A-TCP-R4	F	20	Steel	Steel	600	20:1	Air	25	10	55	0.65	69	[14]
FA-0M	MG	0	Steel	Steel	250	25:1	Air	25	5	60	0.268	88	[15]
FA-5M	MG	5	Steel	Steel	250	25:1	Air	25	2	42	0.64	73	[15]
FA-10M	MG	10	Steel	Steel	250	25:1	Air	25	4	34	0.377	55	[15]
FA-15M	MG	15	Steel	Steel	250	25:1	Air	25	8	46	0.339	70	[15]
FA-20M	MG	20	Steel	Steel	250	25:1	Air	25	12	42	0.527	58	[15]
HA	F	0	Steel	Steel	1200	20:1	Air	600	2	27	0.31	33	[16]
HA	F	5	Steel	Steel	1200	20:1	Air	700	4	35	0.3	42	[16]

Matrix	Reinforcement	Amount of reinforcement%	Type of vial	Type of ball	RPM	BPR	Milling atmosphere	T (°C)	Milling time	Mean grain size(nm)	Elasticity	Crystallinity (X_c)	Ref
HA	F	10	Steel	Steel	1200	20:1	Air	800	6	40	0.35	50	[16]
HA	F	15	Steel	Steel	1200	20:1	Air	900	8	45	0.37	56	[16]
HA	Alumina +TiO2	77	Steel	Steel	400	10:1	N2	1200	2	50	0.621	61	[17]
HA	Alumina+ TiO2	77	Steel	Steel	400	10:1	N2	1250	4	45	0.601	69	[17]
HA	Alumina+ TiO2	77	Steel	Steel	400	10:1	N2	1300	6	40	0.530	48	[17]
FHA1	F	0	Zro2	Zro2	350	35:1	Ar	25	2	44	0.456	39	[18]
FHA2	F	25	Zro2	Zro2	350	35:1	Ar	25	4	36	0.425	35	[18]
FHA3	F	50	Zro2	Zro2	350	35:1	Ar	25	6	35	0.415	27	[18]
FHA4	F	75	Zro2	Zro2	350	35:1	Ar	25	8	30	0.390	31	[18]
FHA5	F	100	Zro2	Zro2	350	35:1	Ar	25	10	32	0.406	28	[18]
HA	zircon	0	Steel	Steel	530	20:1	Air	37	12	29	0.340	22	[19]
HA	zircon	5	Steel	Steel	530	20:1	Air	37	14	28.5	0.335	65	[19]
HA	zircon	10	Steel	Steel	530	20:1	Air	37	18	28	0.327	57	[19]
HA	zircon	15	Steel	Steel	530	20:1	Air	37	20	27.5	0.315	69	[19]
HA	zircon	20	Steel	Steel	530	20:1	Air	37	30	26.5	0.295	62	[19]
HA	zircon	25	Steel	Steel	530	20:1	Air	37	40	26	0.281	60	[19]
NHA	Hardystonite	0%	Steel	Alumina	600	10:1	Air	1130	.33	40	0.537	80	[20]
NHA	Hardystonite	5	Steel	Alumina	600	10:1	Air	980	24	34	0.398	65	[20]
NHA	Hardystonite	10	Steel	Alumina	600	10:1	Air	900	2	39	0.520	69	[20]
NHA	Hardystonite	15	Steel	Alumina	600	10:1	Air	850	4	38.5	0.506	48	[20]
NHA-Di	diopside	10	Steel	Alumina	600	10:1	Air	750	4	33	0.293	55	[21]
NHA-Di	diopside	20	Steel	Alumina	600	10:1	Air	850	8	32	0.280	50	[21]
NHA-Di	diopside	30	Steel	Alumina	600	10:1	Air	950	10	30	0.263	44	[21]
FNHA	zircon	0	porcelain	alumina	400	15:1	Ar	25	2	40	0.393	23	[22]
FNHA	zircon	5	porcelain	alumina	400	15:1	Ar	25	4	36	0.382	20	[22]
FNHA	zircon	10	porcelain	alumina	400	15:1	Ar	25	6	33	0.393	18	[22]
FNHA	zircon	15	porcelain	alumina	400	15:1	Ar	25	8	32	0.359	17	[22]

Table 2. Symbols and description of materials presented in Table 1.

Symbol	Description
HA-R1	R1: $CaHPO_4 + Ca(OH)_2$
HA-R2	R2: $CaCO_3 + CaHPO_4$
HA-R3	R3: $CaHPO_4 + CaO$
TCP	Tricalcium phosphate
A-TCP	Amorphous TCP
A-TCP-R1	R1: $CaO + P_2O_5$
A-TCP-R2	R2: $CaO + CaHPO_4$
A-TCP-R3	R3: $Ca(OH)_2 + P_2O_5$
FA	Fluorapatite
FHA	Fluor-Hydroxyapatite
NHA	Natural-Hydroxyapatite
NHA-Di	Natural Hydroxyapatite Diopside
FNHA	Fluor-Natural-Hydroxyapatite

Their learning algorithm was called back-propagation (BP) and is now the most widely used learning algorithm.

The BP pattern is employed in the present study. It is a highly effective learning means that can be applied to a wide range of problems. The BP associated paradigms require supervised training. This means that they must be educated via a set of training data where known solutions are supplied. BP type neural networks process information in interlinking processing elements (often called neurons, units or nodes; in our study we will use nodes). These nodes are organized into groups labelled as layers. There are three distinct types of layers in a BP neural network: the input layer, the hidden layer, and the output layer. A network encompasses one input layer, one or more hidden layers, and one output layer. There are some relations between the nodes of adjacent layers to relay the output signals from one layer to the next. Fully connected networks occur when all nodes in each layer receive connections from all nodes in each previous layer. The data enter a network through the nodes of the input layer.

4- Neural network model structure and parameters

ANN model used in this research includes thirteen neurons in the input layer and one neuron in the output layer as shown in Fig. 1. This architecture is a 13–9–1 multilayer perceptron (MLP), meaning that it is a network containing three layers including the input layer with thirteen nodes, the hidden layer with nine nodes, and the output layer with one nodes. The values for the input layers were the grain size of HA and HA based nanocomposites obtained at various parameters as mentioned above. The values for the output layer were the mean grain size data in one set. One hidden layer with 9 neurons was used in the architecture of multilayer neural network because of its minimum absolute percentage error values for training and testing sets in Fig. 2. After testing the effect of the number of neurons in the hidden layer on the network performance, the optimal configuration of the ANN model using BP algorithm was found to be 13–9–1.

The neurons of the neighboring layers were entirely interconnected by weights. Finally, the output layer of neurons produces the network anticipation as a result. In this study, the BP training algorithm has been utilized in the feed-forward single hidden layer network. BP algorithm, as one of the most well-known training algorithms for the multilayer perceptron, is a gradient descent technique to diminish the error for a particular training pattern in which it adjusts the weights by a small amount at a time [27]. The non-linear Tangent Hyperbolic (Tanh) activation function was employed in the hidden layer and the neuron outputs at the output layer. The trained model was only tested with the input values and the predicted results were close to the experimental ones.

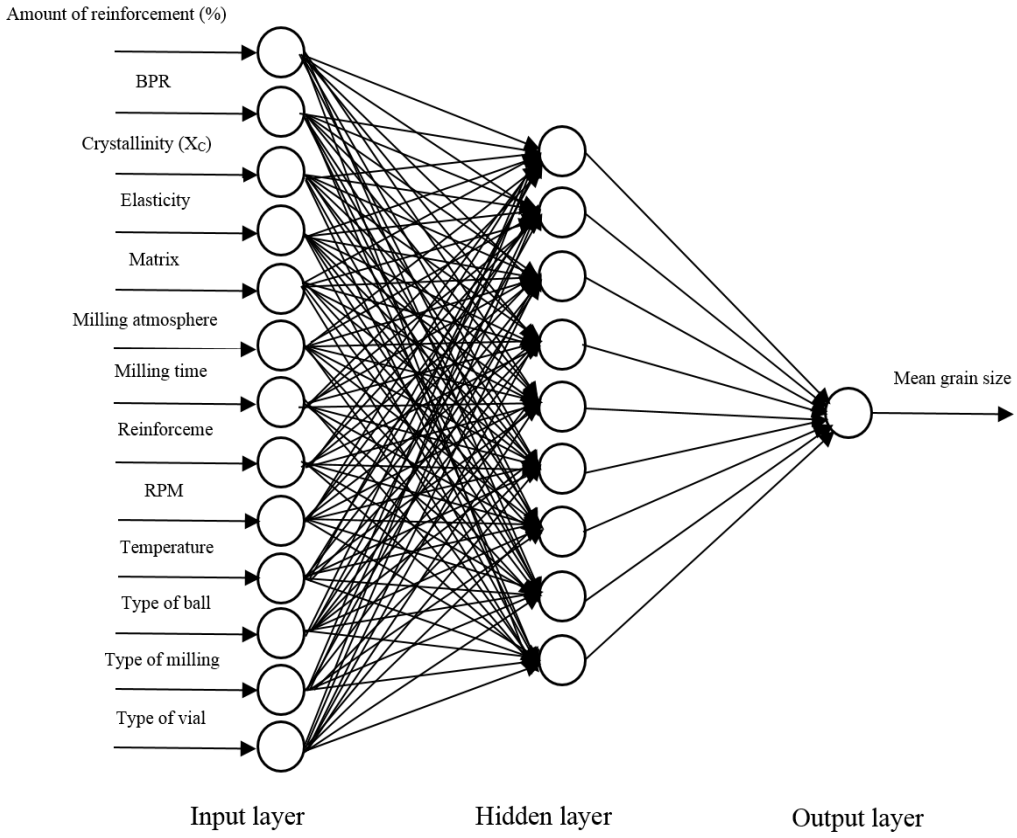

Fig. 1. The MLP neural network architecture used for training and modeling of the mean grain size.

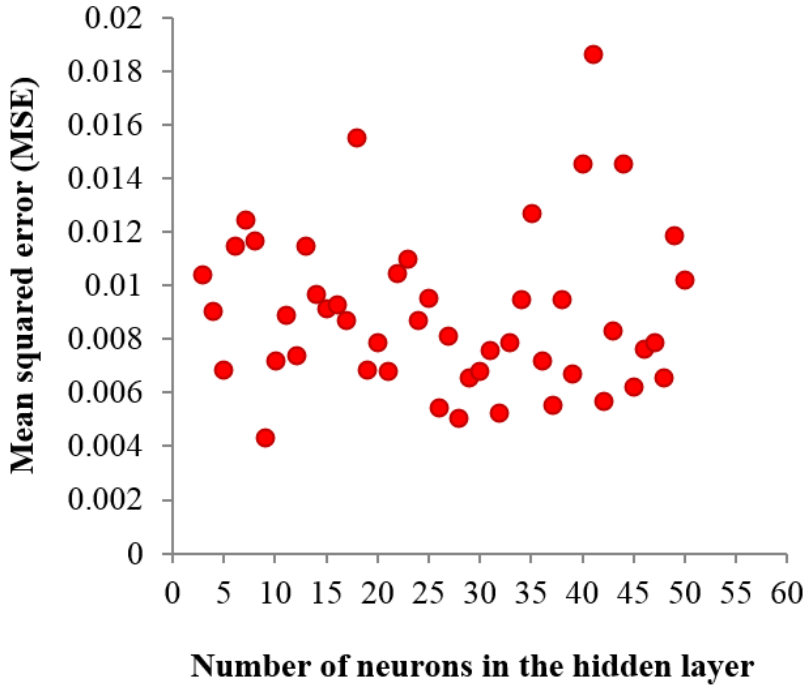

Fig. 2. The MLP neural network normal errors in different networks with different neurons in the hidden layer.

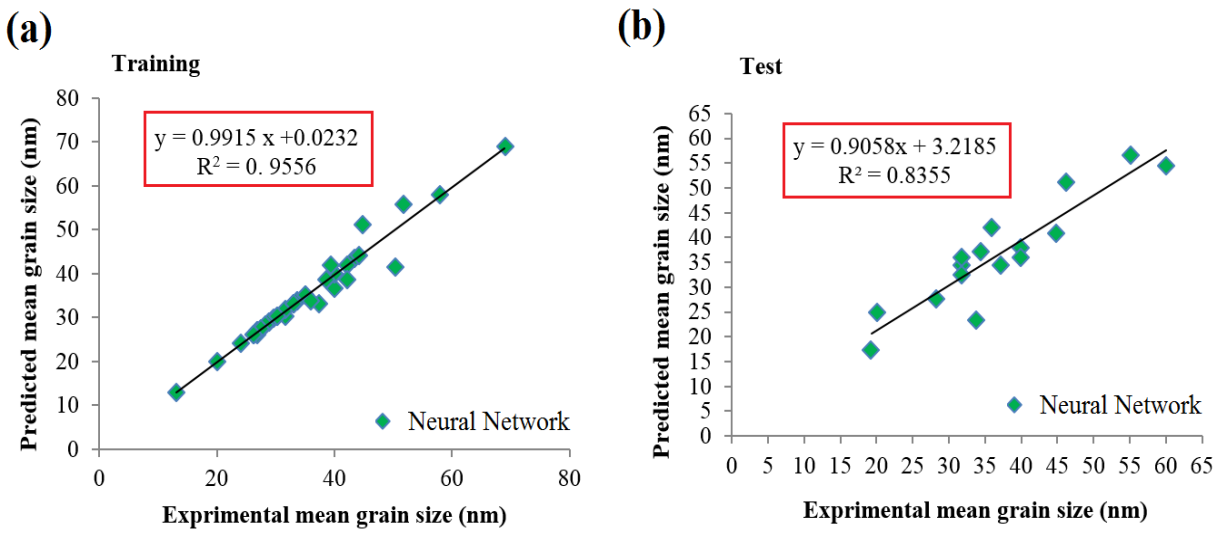

Fig. 3. The correlation of the measured and predicted mean grain size values of the synthesized nanopowders in (a) training and (b) testing phase for neural network model.

The values of parameters used in neural network model are given in Table 3. To make a decision on the completion of the training processes, the termination state is declared as the ANN model, indicating that the training ended when minimum error norm of network was gained.

Table 3. Neural network experimental settings.

Characteristic	Setting network
Type of network	MLP feedforward BP
Learning algorithm	Levenberg Marquardt (LM)
Trigger functions hidden layer	Tangent Hyperbolic (Tanh)
Number of layer	1
Number of neuron	9

5- Discussion and predicted results

One of the most challenging duties in ANN researches is to find this optimal network architecture, which is based on the designation of numbers of optimal layers and neurons in the hidden layers by a trial and error approach. The tasks of initial weights and other related parameters may also affect the performance of ANN to a great extent. However, there is no certain procedure to have an optimal network architecture and parameter settings where the trial and error method still remains valid [28–31].

In this study, Matlab Neural Network toolbox is used for ANN applications. To address the optimization difficulty, a program has been developed in Matlab which automatically handles the trial and error process. The program tries various numbers of layers and neurons in the hidden layer when the highest mean squared error (MSE) of the testing set, as the training of the testing set, is achieved [28–31]. In this study, the error appeared during the training and testing in ANN models can be shown as absolute fraction of variance (R^2) calculated by Equation (1) [32]:

$$R^2 = 1 - \left(\frac{\sum_i (t_i - o_i)^2}{\sum_i (o_i)^2}\right) \quad (1)$$

where t is the target value, o is the output value, and i is the pattern. All of the results obtained from experimental studies and predicted by using the training and testing results of neural network models are given in Fig 3. From Fig. 3, it is inferred that the values obtained from the training and testing in neural network are relatively close to the collected experimental results by an accuracy of more than 96% for the training set and more than 83% for the testing set.

As shown in Fig.3a, the predicted results from models are compared to the collected experimental results for the training sets. The results proved that the proposed model has

moderately well learned the non-linear relationship between the input and the output variables with a good correlation and comparatively low error values. The result of the testing phase in Fig.3b shows that the neural network model is capable of generalizing between input and output variables with reasonably good predictions and accuracy more than 83%. Comparing the neural network model prediction with the collected experimental results for the testing and training stages demonstrates a generalization capacity of the proposed model and fairly low error values. All of these findings exhibit a successful performance of the model for predicting the mean grain size values of the synthesized nanopowders in training and testing stages.

6- Conclusion

In this research, the data collected from previous studies (HA and HA based nanocomposites) were selected. The Artificial Neural Network (ANN) model has been used to predict the mean grain size of Hydroxyapatite from input parameters. The results obtained from the model demonstrated that only multilayer feed-forward neural networks could have a suitable agreement with the other collected results. By using the data, a prediction model was improved by means of artificial neural network to determine the mean grain size of the ball-milling process. In this model, 55 data sets were used so that 40 data sets (73%) were randomly chosen for the training set, and 15 data sets (27%) were used as the testing set. The prediction model demonstrated a very good statistical performance with a 0.84 correlation coefficient between the actual/ modeling data and the network predicted output. For the ranges of the input variables examined, the BP neural network model successfully predicted the mean grain size. This confirmed that the composed prediction model has a high reliability rate. Hence the neural network based prediction model developed in this study can be applied with a high degree of accuracy and reliability for not only determining the mean grain size of HA based bioceramics, but also resulting in large economic benefits for industries.

7- Acknowledgments

The authors are grateful to the research affairs of the Islamic Azad University, Najafabad Branch for supporting this research.

8- Reference

[1] C. Suryanarayana, "Mechanical alloying and milling", Prog. Mater. Sci., vol. 46, 2001, pp. 1-184.

[2] B.B. Khina, F.H. Froes, "Modeling mechanical alloying: advances and challenges." J.O.M, vol. 487, 1996, pp. 36-38.

[3] J.S. Benjamin, T.E. Volin, "The mechanism of mechanical alloying", Metallurgical Transactions, vol. 5, 1974, pp. 1929–1934.

[4] S. Malinov, W. Sha, "Software products for modelling and simulation in materials science", Comput Mater Sci, vol. 28 , 2003, pp. 179-198.

[5] H.K.D.H. Bhadeshia, "Neural networks in materials science", ISIJ Int, vol. 39 , 1999, pp. 966-979.

[6] R.P. Lippmann, "An introduction to computing with neural nets", IEEE ASSP Mag, 1987, pp. 4-22.

[7] L.L. Hench , "Bioceramics: from concept to clinic", J Am Ceram Soc, vol. 74, 1991, pp. 1487-1510.

[8] H. Liu, G.W. Xu, Y.F. Wang, H.S. Zhao, S. Xiong, Y. Wu, B.C. Heng, C.R. An, G.H. Zhu and D.H. Xie, "Composite scaffolds of nano-hydroxyapatite and silk fibroin enhance mesenchymal stem cell-based bone regeneration via the interleukin 1alpha autocrine/paracrine signaling loop", Biomaterials, vol. 49, 2015, pp. 103-112.

[9] N. Altinkok, R. Koker, "Mixture and pore volume fraction estimation in Al_2O_3/SiC ceramic cake using artificial neural networks", Mater Des, vol. 26, 2005, pp. 305-311.

[10] N. Altinkok, R. Koker, "Modelling of the prediction of tensile and density properties in particle reinforced metal matrix composites by using neural networks", Mater Des , vol. 27, 2006, pp. 625-631.

[11] B. Nasiri-Tabrizi, A. Fahami, R. Ebrahimi-Kahrizsangi, "Effect of milling parameters on the formation of nanocrystalline hydroxyapatite using different raw materials", Ceram Inter, vol. 39, 2013, pp. 5751–5763.

[12] A. Fahami, R. Ebrahimi-Kahrizsangi, B. Nasiri-Tabrizi, "Mechanochemical synthesis of

hydroxyapatite/titanium nanocomposite", Solid State Sci, vol. 13, 2011, pp. 135-141.
[13] A. Fahami, B. Nasiri-Tabrizi, R. Ebrahimi-Kahrizsangi, "Synthesis of calcium phosphate-based composite nanopowders by mechanochemical process and subsequent thermal treatment", Ceram Inter, vol. 38, 2012, pp. 6729–6738.
[14] B. Nasiri-Tabrizi, A. Fahami, "Mechanochemical synthesis and structural characterization of nano-sized amorphous tricalcium phosphate", Ceram Inter, vol. 39, 2013, pp. 8657-8666.
[15] M. Kheradmand far, Synthesis and characterization of magnesium-fluorhydroxyapatite coating nanopowders via mechanical alloying, Ph.D. Thesis, Isfahan University of Technology, Iran, 2012.
[16] G. Razi, The effect of the amount and type of nanoceramics reinforcement on the mechanical properties of Co-Cr-Mo alloy using milling machine, Ph.D. Thesis, Isfahan University of Technology, Iran, 2010.
[17] M. Aminzare, A. Eskandari, M.H. Baroonian, A. Berenov, Z.R. Hesabi, M. Taheri, S.K. Sadrnezhaad, "Hydroxyapatite nanocomposites: Synthesis, sintering and mechanical properties", Ceram Inter, vol. 39, 2013, pp. 2197-2206.
[18] M. Zahraie, Preparation and characterization of fluorhydroxyapatite through mechanochemistry and sol-gel methods, Ph.D. Thesis, Isfahan University of Technology, Iran, 2009.
[19] A. Roohani, Synthesis and characterization of Hydroxyapatite nanopowders via mechanical alloying, Ph.D. Thesis, University of Isfahan Technology, Iran, 2013.
[20] H. Gheisari, E. Karamian, M. Abdellahi, "A novel hydroxyapatite–Hardystonite nanocomposite ceramic", Ceram Inter, vol. 41, 2015, pp. 5967-5975.
[21] A. Khandan, M. Abdellahi, R.V. Barenji, N. Ozada, "Introducing natural hydroxyapatite-diopside (NHA-Di) nano-bioceramic coating", Ceram Inter, vol. 41, 2015, pp. 12355-12363.
[22] E. Karamiana, M. Abdellahi, "Fluorine-substituted HA reinforced with zircon as a novel nano-biocomosite ceramic: Preparation and characterization", IJMR, vol. 106, 2015, pp. 1285-1290.
[23] A. Mukherjee, S.N. Biswas, "Artificial neural networks in prediction of mechanical behavior of concrete at high temperature", Nucl Eng Des, vol. 178, 1997, pp. 1-11.
[24] W.S. McCulloch, W. Pitts, A logical calculus of the ideas immanent in nervous activity, Bull Math- Biophys, 1943, p. 115.
[25] F. Rosenblatt, Principles of neuro dynamics: perceptrons and the theory of brain mechanisms, Spartan Books, Washington. DC, 1962.
[26] D.E. Rumelhart, G.E. Hinton, R.J. Williams, "Learning internal representation by error propagation", Nature, Vol. 323, 1986, pp. 533-536.
[27] A.A. Suratgar, M.B. Tavakoli, A. Hoseinabadi, "Modified Levenberg-Marquardt method for neural networks training", World Acad Sci Eng Technol, 2005, pp. 46-68.
[28] I.H. Guzelbey, A. Cevik, A. Erklig, " Prediction of web crippling strength of cold-formed steel sheetings using neural networks", Constr Steel Res, vol. 62, 2006, pp. 962-973.
[29] I.H. Guzelbey, A. Cevik, M.T. Gogus, "Prediction of rotation capacity of wide flange beams using neural networks", Constr Steel Res, vol. 62, 2006, pp. 950-961.
[30] A. Cevik, I.H. Guzelbey, "Neural network modeling of strength enhancement for Cfrp confined concrete cylinders", Build Environ, vol. 43, 2008, pp. 751-763.
[31] A. Cevik, I.H. Guzelbey, "A soft computing based approach for the prediction of ultimate strength of metal plates in compression", Eng Struct, vol. 29, 2007, pp. 383-394.
[32] I.B. Topcu, M. Sarıdemir, "Prediction of compressive strength of concrete containing fly ash using artificial neural network and fuzzy logic", Comput Mater. Sci, vol. 41, 2008, pp. 305–311.